PRINCETON UNIVERSITY

Department of Aerospace and Mechanical Sciences
Gas Dynamics Laboratory

PARTICLE IMPINGEMENT ON A NOZZLE WALL

Sin-I Cheng and Y. Rimon

Report 696
July 1964

PRINCETON UNIVERSITY

DEPARTMENT OF AERONAUTICAL ENGINEERING

No DDC limit

AFOSR 64-1659

PRINCETON UNIVERSITY

Department of Aerospace and Mechanical Sciences
Gas Dynamics Laboratory

PARTICLE IMPINGEMENT ON A NOZZLE WALL

Sin-I Cheng and Y. Rimon

Report 696
July 1964

UNITED STATES AIR FORCE

Office of Aerospace Research

ACKNOWLEDGEMENT

The original work on this report was started, and in considerable measure carried out, under a contract with the Allegany Ballistics Laboratory (NOrd-16640, Subcontract 68). The work was completed with considerable extensions and amplifications under AF 49(638)-1271 monitored by the Air Force Office of Scientific Research of the Office of Aerospace Research.

SYMBOLS

C — A constant in the definition of ψ

C_{pp} — Specific heat of particles

C_{pg} — Gas Specific heat at constant pressure

h — Constant defined in eqn. (26)

I — Impingement integral for the conical method defined in eqn. (6)

I_1 — Impingement integral for the N-S method defined in eqn. (23)

$\bar{K} = \frac{\eta^2 \rho_p}{18}$ — reference time

K_o — Dimensionless small parameter of momentum transfer

K_H — Dimensionless small parameter of heat transfer

L — Length of the convergent part of the nozzle

N — Coordinate perpendicular to streamlines in Section 4

$P = \frac{2W}{Y} \cdot 100$ — Impingement percentage

q — Magnitude of velocity in Sections 3, 4 and 5

r — Radial coordinate in the conical method, Section 3

t — Dimensional time

U — Axial component of velocity in Section 5

V — Transverse (normal to the axis) component of velocity in Section 5

W	Width of impingement band
$x = r_o - r$	Radial coordinate measured from the entrance in Section 3. Axial coordinate in Section 5.
y	Radial coordinate in the transverse plane
Y	Vertical coordinate of nozzle wall
z	Non-dimensional time
α	Non-dimensionalization constant of ψ
γ	Gas specific heats ratio = C_{pg}/C_{vg}
γ_i	Equivalent isentropic specific heats ratio in zeroth order solution
η	Particles diameter
θ	Angle coordinate in Section 3
θ	Originating angle of the particle which hits the throat in Sections 3, 4
Θ	Nozzle wall angle in conical method Section 3
λ	Gas-particles mass flux ratio
μ	Gas viscosity
ρ	Density
ω	Mass flux

Subscripts

0	Entrance conditions
c	Conical
g	Gas
N	Properties in direction N
S	Properties in direction S

N.S. Properties of the N-S method

p Particles

r Radial

t Throat

θ Tangential

2D Properties of the two-dimensional method

Superscripts

* Combustion chamber properties

Barred symbols are dimensional quantities

SUMMARY

The percentage of the mass flux of fine particles carried in a two phase fluid that impinge on the wall of the convergent section of a nozzle is investigated with many different methods, to reveal the qualitative trends of different physical factors.

If the particles are uniformly distributed over the nozzle entrance and if the diameter of the particles is less than 5 microns, the particles in the turbulent core outside the displacement area of the turbulent boundary layer on the wall of of the rocket chamber will pass through. The percentage of particle mass flux that impinges on the nozzle wall is very small.

Qualitatively, it is concluded that:

(a) Most of the impingement takes place in the entrance region, where the heat transfer condition is not so severe as is in the throat region. The percentage mass flux of particle impingement is insensitive to nozzle shape near the throat but depends heavily on the nozzle geometry near the entrance.

(b) The effect of moderate changes in γ of the gas is negligible.

(c) Increase in particle dispersed density causes slight decrease in percentage of impingement, but the absolute amount of impingement is increased.

(d) For the same nozzle geometry and particle concentration, the amount of impingement is directly proportional to the particle diameter squared.

(e) Increase in the convergence angle of the nozzle causes an increase in the percentage of the impingement.

TABLE OF CONTENTS

1. INTRODUCTION

In many modern solid propellant rockets, metallic powders like aluminum are added to the propellant. The metallic oxides are found in the combustion chamber as condensed phases, either as liquid droplets or as solid particles of micron sizes. The two phase fluid expands through the rocket nozzle with complicated processes of heat and momentum transfer between the particles and the gas. The condensed oxide particles (or droplets) are much hotter than the expanding gas. An impingement of a hot particle on the nozzle wall will not only decrease the thrust-producing outgoing momentum, but will also increase the heat transfer to the wall. The latter aggravates the heat transfer conditions on the converging wall of the nozzle where the gaseous heat transfer is already quite severe.

It is therefore of interest to estimate the percentage of impingement of the particle mass flux on the wall, small as it may be, and to find the various parameters of significance.

The various aspects of the interaction phenomena between the condensed and the gaseous phases and the calculation of the thermodynamic and dynamic properties of the gas and particles are discussed in detail in Reference 1. The results and method of calculation of Reference 1 is adopted here for investigating the impingement phenomena. Accordingly, the

following assumptions and restrictions made in Reference 1 are adopted:

(a) Small perturbation method. The convergence of the solution is good only for small values of the small disturbance parameters K_o and K_H.

(b) Quasi one-dimensional assumption of gaseous flow.

(c) Uniform distribution of particles without interparticle collisions.

(d) Stokes drag law holds for the micron size particles.

We propose to use several different approximate methods for investigating the impingement phenomena to reveal the relative significance of different physical factors. Numerical calculations of the differential equations systems governing the impingement will also be performed to estimate the overall effect.

2. THE CONICAL APPROXIMATION

As a first attempt we shall make the following assumptions, in addition to, or as an amplification of those made already in Reference 1.

(a) The gas flow is purely conical, i.e., the gas streamlines are rays emanating from a vertex downstream of the throat.

(b) This conical flow is valid from the entrance of radius r_o to the point N where the tangent to the geometric throat of the nozzle meets the extrapolated conical approximation to the nozzle contour (see Figure 1).

(c) The thermodynamic and flow properties of both the gas and the particles are constant along circular arcs whose center is in the vertex of the conical surface.

(d) The particles will possess a velocity component perpendicular to the conical element, i.e., a tangential component. There will be no azimuthal velocity component (at least on the average). The radial velocity of the gas and the particle on each arc defined by x (see Figure 1) are those determined at that x by the one-dimensional analysis in Reference 1.

(e) The velocity of the particles at the entrance to the nozzle is parallel to the nozzle axis, i.e., the initial tangential velocity component of the particle is

$$q_{p\theta 0} = q_{pr0} \cdot tg\theta_o$$

(see Figure 1).

We shall non-dimensionalize all velocities by the speed of sound in the combustion chamber q^*, all lengths by the length of the converging section of the nozzle L, and time by a reference time

$$\bar{K} = \frac{\eta^2 \rho_p}{18\mu}$$

thus we get:

$$s = \frac{\bar{x}}{L} \qquad r_o = \frac{\bar{r}_o}{L} \qquad r_t = \frac{\bar{r}_t}{L} \qquad r = \frac{\bar{r}}{L}$$

$$q_g = \frac{q_g}{q^*} \qquad q_p = \frac{q_p}{q^*} \qquad z = \frac{t}{\bar{K}}$$

The dimensionless equations of motion of the particles in the r and θ directions are (see Reference 2):

$$\frac{dq_{pr}}{dz} = q_g - q_{pr} \tag{1}$$

$$\frac{dq_{p\theta}}{dz} = - q_{p\theta} \tag{2}$$

Centrifugal terms in eqns. (1) and (2), like $\frac{q_{p\theta}^2}{r}$ or $\frac{q_{p\theta}q_{pr}}{r}$ were neglected. It was checked and found that these terms did not exceed 1% of the terms retained. Also, the assumption (c) was used in putting $\frac{\partial}{\partial\theta} = 0$. By integrating eqn. (2) and defining $q_{p\theta}$ as

$$q_{p\theta} = \frac{L}{u^*\bar{K}} \cdot r \frac{d\theta}{dz}$$

one gets:

$$d\theta = K_o q_{p\theta o} \cdot \frac{1}{r} e^{-z} dz \qquad (3)$$

where

$$K_o = \frac{\bar{K}q^*}{L}$$

is the dimensionless parameter of small perturbation in Reference 1, and $q_{p\theta o}$ is the initial tangential velocity of the particle. We shall find the angle θ_o from which the particle passing through the point N originated. The area percentage of the annular region of width W_c (Figure 1) determined by θ_o, gives a close upper bound of the percentage of particle flux impinging on the converging nozzle wall:

$$P_c = \frac{2\pi Y_o W_c}{\pi Y_o^2} \cdot 100 = \frac{2W_c}{Y_o} \cdot 100 \qquad (4)$$

With $r = r_o - x$ and

$$q_{pr} = \frac{1}{K_o} \frac{dx}{dz}$$

together with our assumption (e) for $q_{p\theta o}$, eqn. (3) becomes

$$d\theta = q_{pro} \cdot tg\theta_o \cdot \frac{e^{-\frac{1}{K_o}\int_o^x \frac{dx}{q_{pr}}}}{(r_o - x) q_{pr}} dx \qquad (5)$$

By integrating eqn. (5) from θ_o to Θ and denoting $X = r_o - r_t$ and

$$\int_o^X \frac{e^{-\frac{1}{K_o}\int_o^x \frac{dx}{q_{pr}}}}{(r_o - x)\, q_{pr}} dx = I \qquad (6)$$

one gets finally

$$\Theta - \theta_o - q_{pro} \cdot tg\theta_o \cdot I = 0 \qquad (7)$$

For a given conical nozzle and known values of K_o and q_{pro}, I can be evaluated and Θ is known. Eqn. (7) can be solved for θ_o either graphically or by trial and error.

For an approximate solution of θ_o when Θ is small take $tg\theta_o = \theta_o$ thus

$$\theta_o \approx \Theta (1 - q_{pro} \cdot I) \qquad (8)$$

also

$$W_c = r_o(\sin\Theta - \sin\theta_o) \cong r_o(\Theta - \theta_o) \qquad (9)$$

using eqns. (8) and (9) in (4) we get:

$$P_c \cong \frac{2r_o \cdot \Theta \cdot q_{pro} I}{Y_o} \cdot 100 \qquad (10)$$

as an approximate expression for the impingement percentage.

Since the calculated profiles q_{gr} and q_{pr} are taken numerically as functions of r such as the result of the computation in Reference 1, it is possible (a) to continue directly the numerical program and evaluate I by machine computation, or (b) q_{pr} may be approximated by a polynomial of some degree and then integrated termwise analytically. Eqn. (10) will give an estimate of the impingement percentage. This approximate method is probably adequate when a substantial portion of the converging nozzle is approximately conical.

3. THE N-S METHOD

In this section we shall adopt the streamlines of the gas N = const. and their orthogonal lines S = const. as the coordinate system (see Figure 2). This N-S coordinate system offers substantial improvement over the previous conical approximation near the entrance and near the throat. We shall first keep the same initial flow conditions entering the nozzle for estimating the initial tangential velocity of the particle in order to focus our attention on the role of the shape of the throat.

The one-dimensional gas and particle properties, either thermodynamic or fluid mechanical, as calculated in Reference 1, will be assumed to apply along S = const. lines, i.e. along lines perpendicular to the gas streamlines. Following a procedure similar to that adopted in the conical approximation, we can determine the path and coordinate N (or ψ_o defined in eqn. (15)) of the particle at the initial section, which hits the wall at the throat. N or ψ_o determine W_S (see Figure 2) which, under the assumption of uniform particle distribution across the nozzle section, gives the impingement percentage as

$$P_{N.S.} = \frac{2\pi Y_o W_{N.S.}}{\pi Y_o^2} \cdot 100 = \frac{2W_{N.S.}}{Y_o} \cdot 100 \qquad (11)$$

Equations (1) and (2) written in the N-S coordinates become:

$$\frac{dq_{ps}}{dz} = q_{gs} - q_{ps} \tag{12}$$

$$\frac{dq_{pN}}{dz} = -q_{pN} \tag{13}$$

Again the centrifugal terms in eqn. (12) and (13) were neglected for the same reasons given in eqn. (1) and (2). The integral of eqn. (13) with the use of the assumption of

$$q_{pNo} = q_{pso} \cdot tg\theta_o$$

gives

$$q_{pN} = \frac{1}{K_o} \frac{dN}{dz} = q_{pso} \cdot tg\theta_o \cdot \ell^{-z} \tag{14}$$

Let us define ψ as the stream function of the gas by:

$$d\bar{\psi} = \bar{\rho}_g(s) \cdot \bar{q}_g(s) \cdot c \cdot d(\bar{N}^2) \tag{15}$$

non-dimensionalization with

ω_g = mass flow rate of gas

ρ^* = gas density in combustion chamber

q^* = sonic velocity in combustion chamber

L = length of converging part of the nozzle

gives

$$d\psi = 2c\omega \cdot \rho_g(s) q_g(s) \cdot N dN \tag{16}$$

where

$$\alpha = \frac{\rho_r q^* L^2}{\omega_g}$$

with $\psi = 0$ on the centerline, and $\psi = 1$ on the nozzle wall. At any point in the nozzle defined by ψ and S we have the relation:

$$\left[\frac{N(s,\psi)}{N(s,1)} \right]^2 = \frac{\psi}{1.0} \qquad (17)$$

also

$$d\psi = \frac{\partial \psi}{\partial N} \cdot \frac{dN}{dz} \cdot dz \qquad (18)$$

Using eqns. (17), (16) and (14) in (18) and if we use the radius y instead of the arc length N with less than 1% error for cone angles less than 20° (see Figure 2) we have $C = \pi$ in (16) one finally arrives at:

$$d\psi = 2\pi\alpha \cdot k_o \cdot q_{po} \, tg\theta_o \cdot \rho_g(S) \cdot q_g(S) \cdot N(S,1) \cdot \psi \cdot \ell^{-z} dz \qquad (19)$$

Using again $y(S,1)$ instead of $N(S,1)$ we get from the definition of ψ :

$$\rho_g(S) \cdot q_g(S) \cdot \pi \cdot y(S,1)^2 \cdot \alpha = 1 \qquad (20)$$

By integrating eqn. (19) from ψ_o to 1.0, with the help of eqn. (20), one gets:

$$\frac{1-\sqrt{\psi_o}}{q_{psc}\,tg\theta_o} = \int_o^{z_1} \frac{k_o \cdot \ell^{-z}}{y(S,1)}\,dz = I_1 \qquad (21)$$

Z_1 is the time needed for the particle which starts at ψ_o to reach the throat. Changing the variable in I_1 from z to S through the definition of q_{ps} as :

$$z = \int_o^S \frac{dS}{K_o q_{ps}} \qquad (22)$$

we get for I_1 :

$$I_1 = \int_o^{S_{throat}} \frac{e^{-\frac{1}{K_o}\int_o^S \frac{dS}{q_{ps}}}}{y(S,1)\cdot q_{ps}}\,dS \qquad (23)$$

I_1 must usually be evaluated numerically because of the appearance of $y(S,1)$, which expresses the known nozzle contour.

Once I_1 is evaluated, eqn. (21) must be solved for ψ_o . From the definition of ψ we have, at the entrance section:

$$\psi_o = \alpha \cdot \rho_g(0) q_g(0) \cdot A_o \qquad (24)$$

where $A_o = 2\pi r_c^2(1-\cos\theta_o)$ is the spherical entrance area (see Figure 2) which results in

$$\cos\theta_o = 1 - \frac{\psi_o}{h} \tag{25}$$

where

$$h = \alpha\rho_g(0)q_g(0)\cdot 2\pi r_o^2 = 2\left(\frac{L}{Y_o}\right)^2 \cdot r_o^2 \tag{26}$$

The second expression for h employs the definition of α .

Eqn. (21) for the solution of ψ_o becomes:

$$1 - \psi_o - q_{pso}\cdot I_1 \cdot \sqrt{\frac{\psi_o}{h} + 3\left(\frac{\psi_o}{h}\right)^2} = 0 \tag{27}$$

where q_{pso} and h are known for a certain problem and I_1 has to be evaluated from eqn. (23).

4. TWO-DIMENSIONAL ENTRANCE ANALYSIS

Comparison between the results in the two previous sections serves only to illustrate the function of the throat shape. Since the same approximation of "conical" entrance condition is employed. With a major part of the impingement taking place in the entrance region (to be shown later). We have to investigate carefully the significance of the geometry of the entry section. To facilitate comparison with previous results we shall not, however, attempt a strictly axisymmetric analysis. We shall take the gas velocity q_g near the entrance (see Figure 3) to be that calculated by the use of the one-dimensional small perturbation analysis in Reference 1. Since the area variation near the entrance is small, this is a very good assumption. Adopting the cylindrical polar coordinates (x,y) we write the equations of axial (x) and transverse (y) momentum balance of the particles as:

$$u_p \frac{du_p}{dX} = \frac{1}{K_o}(u_g - u_p) \tag{28}$$

$$u_p \frac{dv_p}{dX} = \frac{1}{K_o}(v_g - v_p) \tag{29}$$

In order to solve (28) and (29) for the particle velocity components u_p and v_p, we must find appropriate expressions for the gas velocity components u_g and v_g. Since the angular deflection of the gas streamlines is small, i.e. β is small, we may write

$$u_g = q_g \cos\beta \cong q_g \tag{30}$$

q_g is known from the one-dimensional small perturbation analysis of Reference 1. The transverse velocity component of gas (perpendicular to the nozzle axis) is:

$$v_g = u_g \, tg\beta = u_g \frac{dy(x)}{dx}$$

From continuity considerations and the definition of the stream function ψ we get:

$$\frac{y(x)}{Y(x)} = \frac{y_o}{Y_o} \tag{31}$$

(see Figure 3). Using eqns. (31) in (30), we get:

$$v_g = u_g \cdot \frac{y_o}{Y_o} \cdot \frac{dY(x)}{dx} \tag{32}$$

$Y(x)$ is a given contour function; thus U_g and v_g are known functions of X and a parameter y_o which is the point where the gaseous element originates. With the help of eqns. (30) and (32), the system of two ordinary differential equations (28) and (29) serve to determine U_p and v_p as functions of x and the parameter y_o. To solve eqns. (28) and (29) by power series is tedious and inaccurate.

They are, hence, solved simultaneously on a computing machine as a part of the program in evaluating q_g from the small perturbation method following Reference 1. Once u_p and v_p are known, they can be integrated in the same program to give the position and direction of the particle at any station x as a function of the parameter y_o as :

$$y_p = y_{po} + \int_o^x \frac{v_p(x,y_o)}{U_p(x,y_o)}\,dx = y_{po}\left(1+\frac{1}{Y_o}\cdot C\right) \qquad (33)$$

where C is a constant and found by the evaluation of the integral, and

$$\phi = \text{arc tg}\left(\frac{v_p}{U_p}\right) \qquad (34)$$

The percentage of impingement upstream of some station X is found by determining the y_o of the particle which hits the wall at that X . This y_o will be denoted by y_{po} . To find y_{po} we put at some X , $y_p = Y(\lambda)$ and from eqn. (33) we have

$$y_{po}(X) = \frac{Y(X)}{1+\frac{1}{Y_o}C} \qquad (35)$$

y_{po} determines W_{2D} the width of impingement region and again we have the impingement percentage as

$$P_{2D} = \frac{2W_{2D}}{Y_o}\cdot 100 \qquad (36)$$

5. RESULTS AND COMPARISON OF THE VARIOUS METHODS

From the studies done in the previous sections and in Reference 1, we see that the important parameters entering the formulation of the impingement are:

$$\gamma \ , \ \gamma_i \ , \ \lambda \ , \ K_o \ , \ K_H \ , \ \frac{\eta^2}{L}$$

and the geometry of the nozzle. Throughout the calculation two inconsequential assumptions were made in addition, for the sake of simplicity. These are:

(a) $C_{pp} = C_{pg}$ gas and particle specific heats are equal, which implies that $\sigma = \lambda$ in the small perturbation analysis.

(b) $K_o = K_H$ the small perturbation parameter for momentum and heat transfer are equal. All small perturbations were calculated to the first order.

In order to follow the effect of each individual parameter, and to assess the validity of each method, many cases were calculated with results summarized in Table I. Before analyzing the results, let us first get some idea as to the range of sizes of the particles for which our analysis may be applicable. Let us calculate η for a typical value of $k = 0,1$ $L = 4"$, $\rho_p = 1.72$ grams/cm^3, $\mu = 6 \times 10^{-4}$ poise, $U_r = 10,000$ cm/sec. Using this in

$$\eta = \sqrt{\frac{K_c \cdot 18\mu \cdot L}{\rho_p \cdot q_r}}$$

one gets η to be $\eta \cong 8$ microns. The particle sizes corresponding to other values of K_o in a nozzle with the same L are given as $\eta = \eta_{K_o=0,1} \cdot \sqrt{\frac{K_o}{0,1}}$. Our range of interest is hence limited to particles of only several microns in size (less than 13).

A comparison between cases (1) and (2) brings out the first important result. The results obtained in case (1) using the conical method and those in case (2) using the N-S method, are the same. Since these two methods differ only in the throat region, we conclude that the impingement is insensitive to the nozzle shape near the throat. This fact can be explained by the small relaxation distance of the exponential decay of the tangential velocity expressed by eqns. (3) and (14). Because of this rapid decay, the impingement takes place mainly in the entrance section where Z is small. The particle motion soon follows the gas motion upon leaving the entrance. Sizeable changes in the nozzle shape near the throat do not change appreciably the percentage of impingement. This was further demonstrated in the detailed results of the numerical computations of cases (3) to (20).

Since the impingement results for particles of sizes ranging from 5-13 microns depend heavily on the velocity variations

of the gas and the particles in the entrance region, it is necessary to determine accurately the gas and the particle motion in the entrance region. The method of area perturbation as is adopted in Reference 1 is inadequate for the present purpose Accordingly, cases (3) to (20) were calculated for a prescribed nozzle shape (with no area perturbation), step by step with the help of an IBM 7090 high speed computing machine.

Analysis of the results of these cases shows:

(a) Moderate changes in γ have no significant effect on the impingement. This is demonstrated by cases (3) and (4) where γ is the only changing parameter. The results of these two cases are essentially the same.

(b) An increase of the particle mass flux ratio λ in cases (5) to (8) slightly decreases the percentage of impingement. This is due to more heat and momentum transfer between the gaseous and particle phases, which affect the gaseous velocity.

(c) When dealing with a prescribed nozzle geometry, the most important parameter affecting the amount of impingement is the particle diameter η . The effect of η can be detected in cases (9) to (14) where the only varying parameter is $K_o = K_E$. As was shown before for a fixed nozzle geometry η is proportional to $\sqrt{K_o}$. The results of cases (9) to (14) show linear dependency of I , which determines the impingement, on K_o . This is an obvious consequence of the linearized treatment of Reference 1. Therefore, for a given nozzle the impingement percentage is directly proportional to the square of the diameter of particles.

(d) Cases (10) to (12) and (15) to (20) give the effect of the increase in convergence angle of the nozzle from 20° to 40°. As expected, we see that impingement increases with an increase of convergence angle.

Although the approximate conical method is relatively simple, the two-dimensional method yields more consistent results. We see that in Nozzle 1 (cases 3-14) the conical results are almost always higher than the "two-dimensional" results while in Nozzles 2 and 3 (cases 15-20) they are lower. This again can be explained by the rapid decay of tangential velocity in the "two-dimensional" analysis. It is clear that the latter where impingement takes place in 0.4-0.5 of the nozzle length will be more sensitive to increase in convergence angle than the conical method where impingement is negligible after 0.1 of the nozzle length.

All the results summarized in Table I show in common that the overall percentage of particle mass flux that impinge on the nozzle wall is very small. In the range of interest up to $K_o = 0.2$, the impingement width W is of order of magnitude of the displacement thickness of the turbulent boundary layer on the chamber wall at the nozzle entrance. In the boundary layer, the velocities of the gas and the particles are less than those given by the quasi one-dimensional results. The relaxation distance for the transverse velocity component of particle will be accordingly smaller and the particles will follow more closely the

gas streamlines with less impingement. Hence, the present results of small total particle impingement is actually an upper bound. In this case, we may consider our results as an upper bound for the impingement, and conclude that in this size range impingement is negligible.

When interpreting cases (17) to (20) where the impingement is somewhat greater, we should bear in mind that the values of K_o are rather large and the validity of the linear perturbation results is questionable. These cases were included mainly to show a qualitative trend.

REFERENCE

1. Chiu, H. H.: One-dimensional Heterogeneous Two-phase Flow in Rocket Nozzles. Princeton University Department of Aerospace & Mechanical Sciences Ph.D. Thesis, 1962.

TABLE 1

No.	Nozzle	Method	$K_o=K_E$	$\lambda=6$	γ	γ_1	I	$W_{c[in]}$	$W_{T.D_{[in]}}$	P_c	$P_{T.D}$
1	0	conical analytically	0.1	0.4	1.3	1.2		0.01076		1.0	
2		M-6 numerically	0.1	0.4	1.3	1.2		0.0107		1.0	
3			0.1	0.4	1.2	1.15	0.072470	0.019	0.018	1.9	1.8
4		conical	0.1	0.4	1.3	1.2	0.072458	0.0155	0.0176	1.85	1.76
5		and	0.1	0.1	1.3	1.2	0.07295	0.021	0.020	2.10	2.0
6		T.D.	0.1	0.2	1.3	1.2	0.072513	0.020	0.0196	2.0	1.96
7		computed	0.1	0.3	1.3	1.2	0.072484	0.019	0.0188	1.9	1.9
8	1	numerically	0.1	0.4	1.3	1.2	0.072458	0.155	0.0176	1.55	1.76
9			0.05	0.4	1.3	1.2	0.036137	0.009		0.9	0.0
10			0.10	0.4	1 3	1.2	0.072458	0.155	0.176	1.55	1.76
11			0.20	0.4	1.3	1.2	0.14633	0.038	0.0392	3.8	3.92
12			0.30	0.4	1.3	1.2	0.22[illegible]8	0.060	0.0588	6.0	5.9
13			0.40	0.4	1.3	1.2	0.29942	0.084	0.0772	8.4	7.72
14			0.50	0.4	1.3	1.2	0.37919	0.108	0.0936	10.8	9.36
15			0.10	0.4	1.3	1.2	0.066180	0.017	0.0246	1.7	2.46
16	2	conical + T.D.	0.20	0.4	1.3	1.2	0.13354	0.036	0.0465	3.6	4.65
17			0.30	0.4	1.3	1.2	0.20226	0.056	0.0666	5.6	6.6
18			0.10	0.4	1.3	1.2	0.071864	0.019	0.0341	1.95	3.4
19	3	conical + T.D.	0.20	0.4	1.3	1.2	0.14512	0.040	0.0605	4.0	6.0
20			0.30	0.4	1.3	1.2	0.21999	0.063	0.0842	6.3	8.4

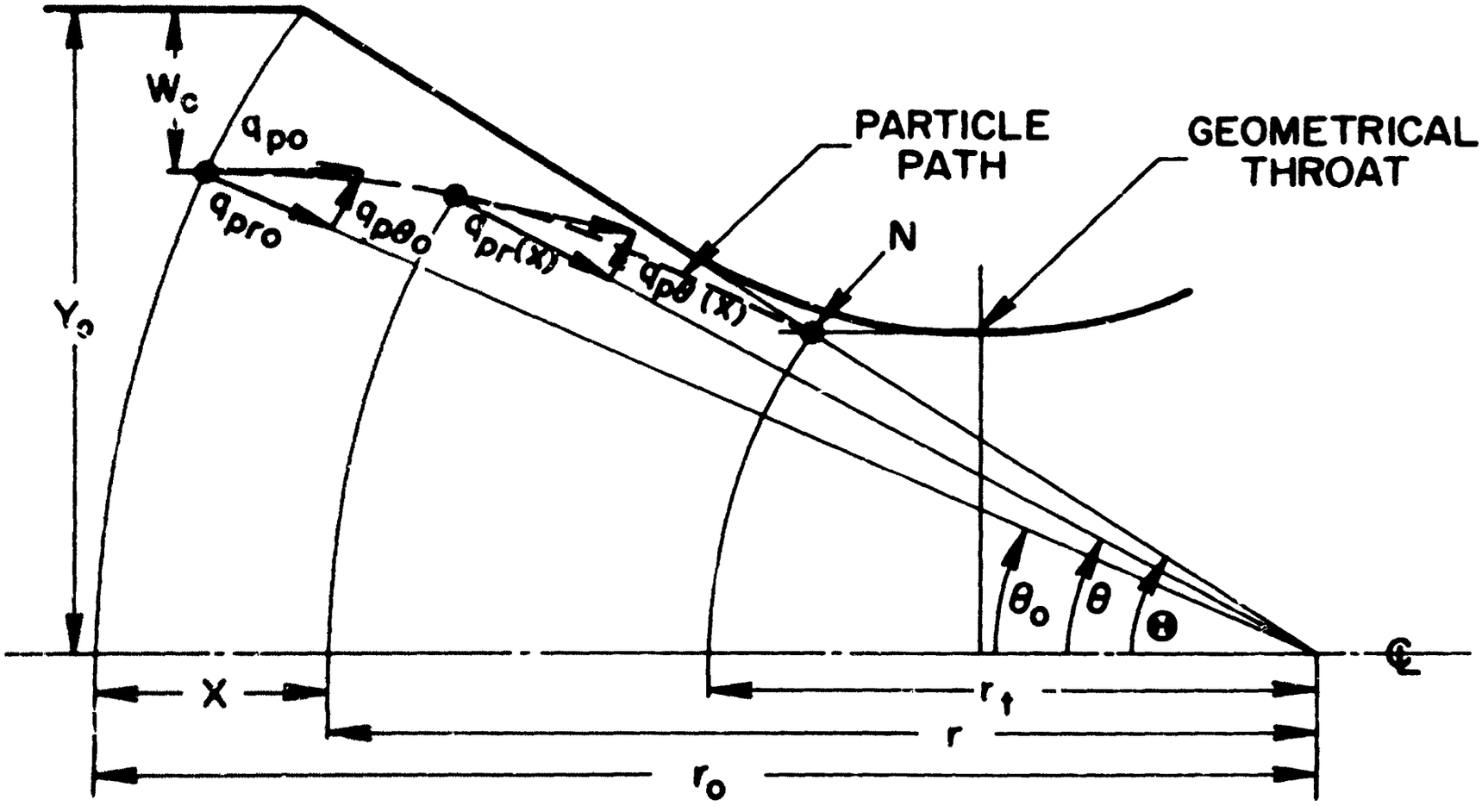

IV M3-1

Figure 1. The conical coordinates

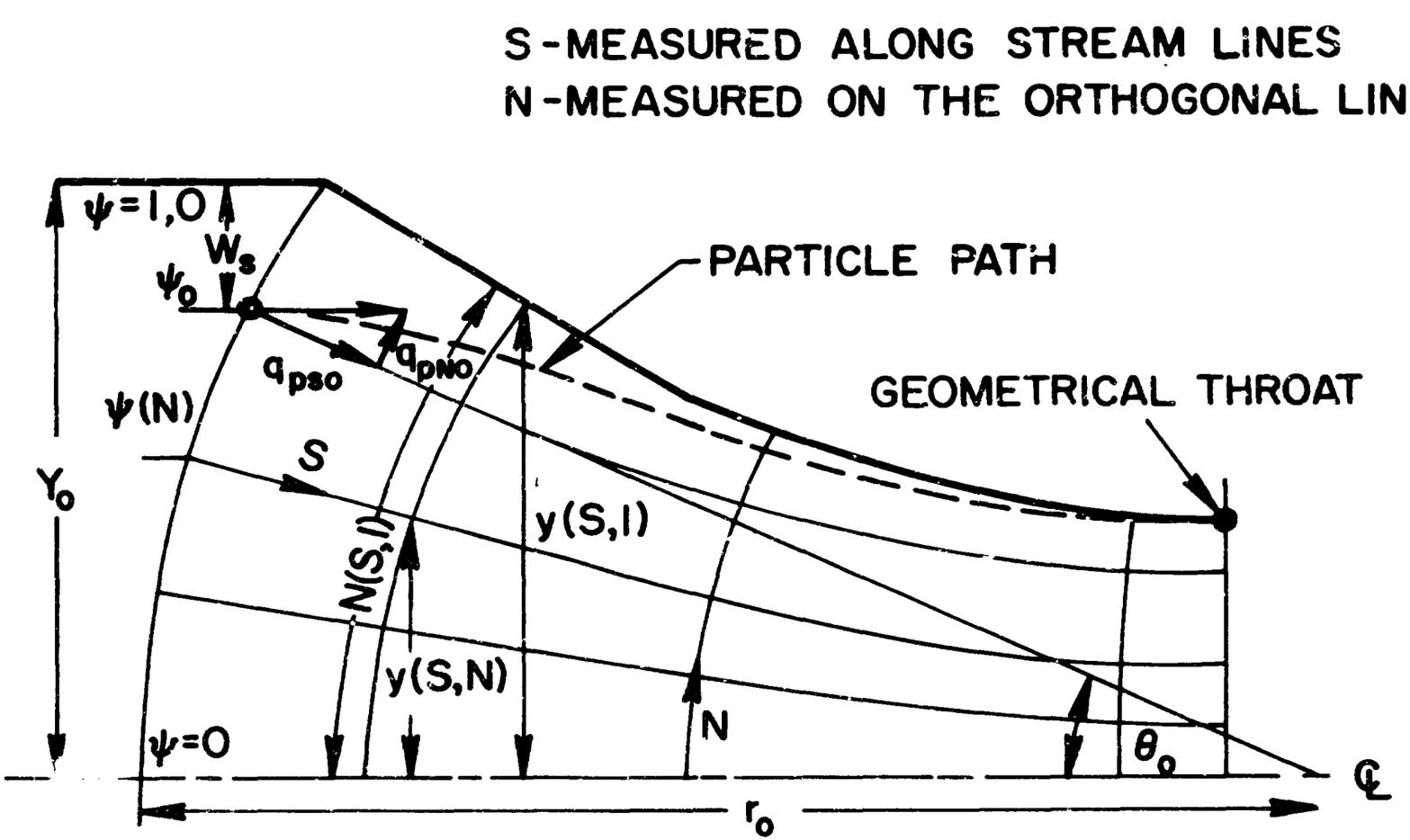

IV M3-2

Figure 2. The N-S coordinates

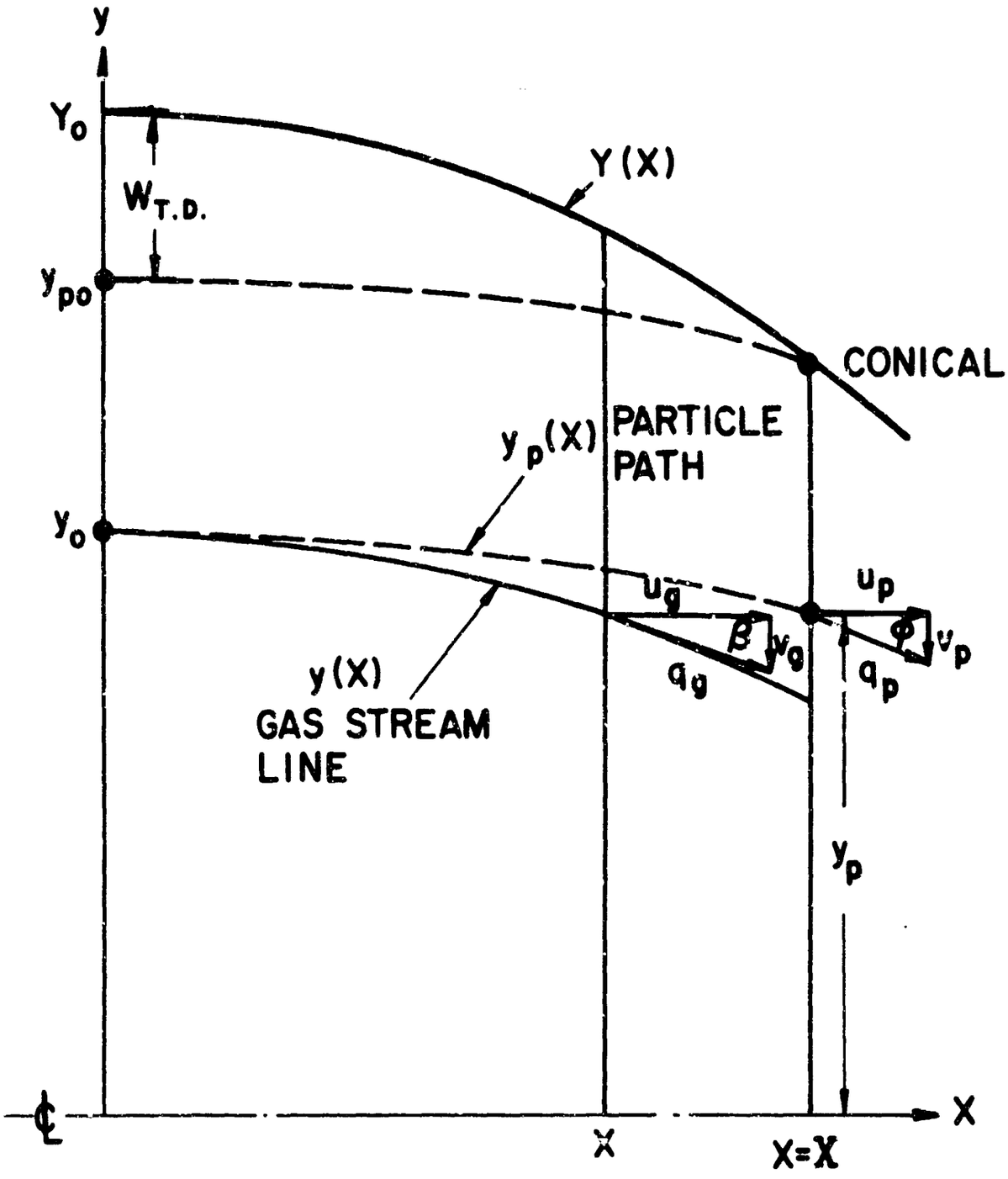

IV M3-3

Figure 3. Two-dimensional analysis

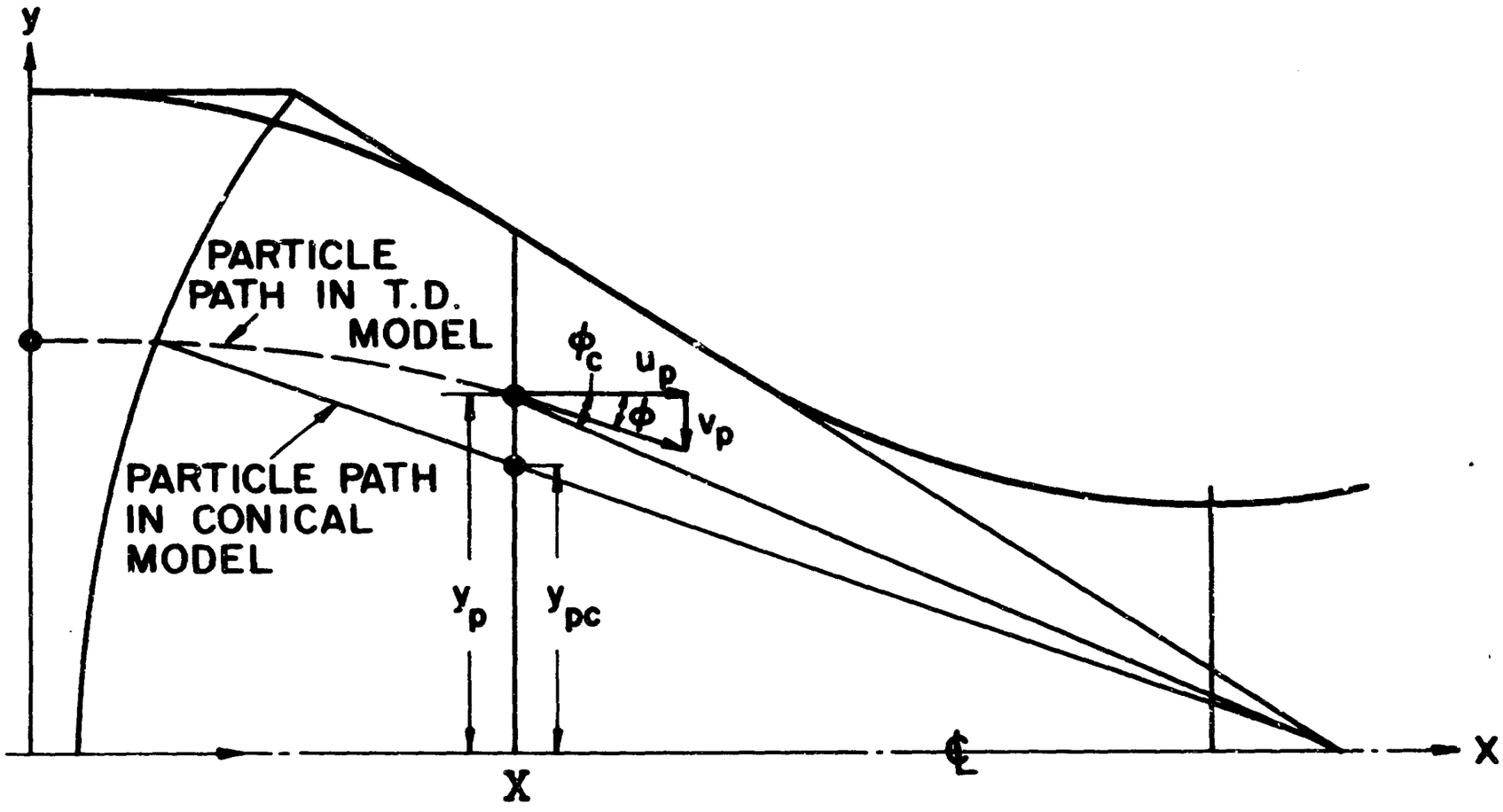

IV M3-4

Figure 4. Comparison between conical and two-dimensional methods

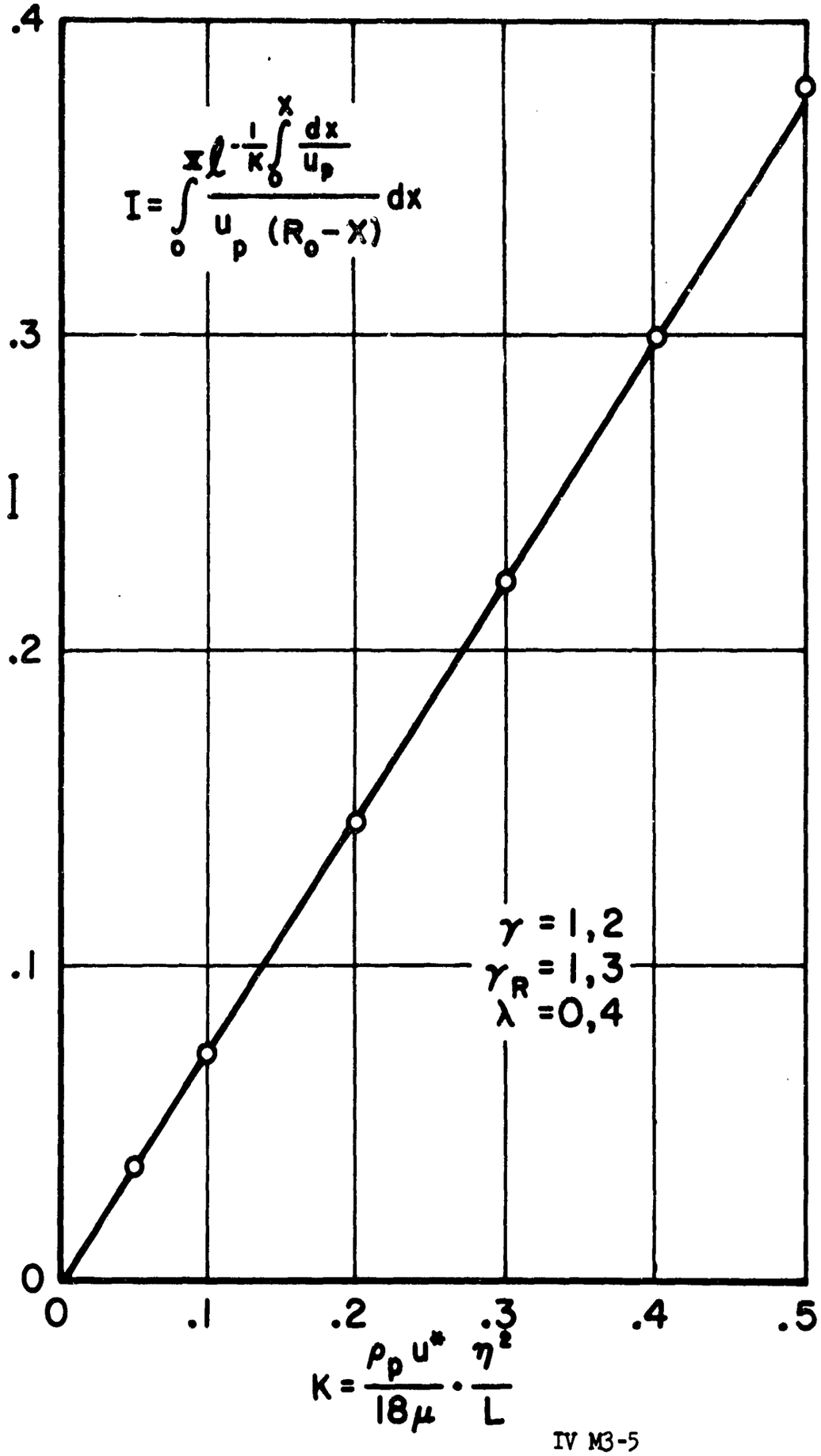

Figure 5. Impingement vs. small parameter K .

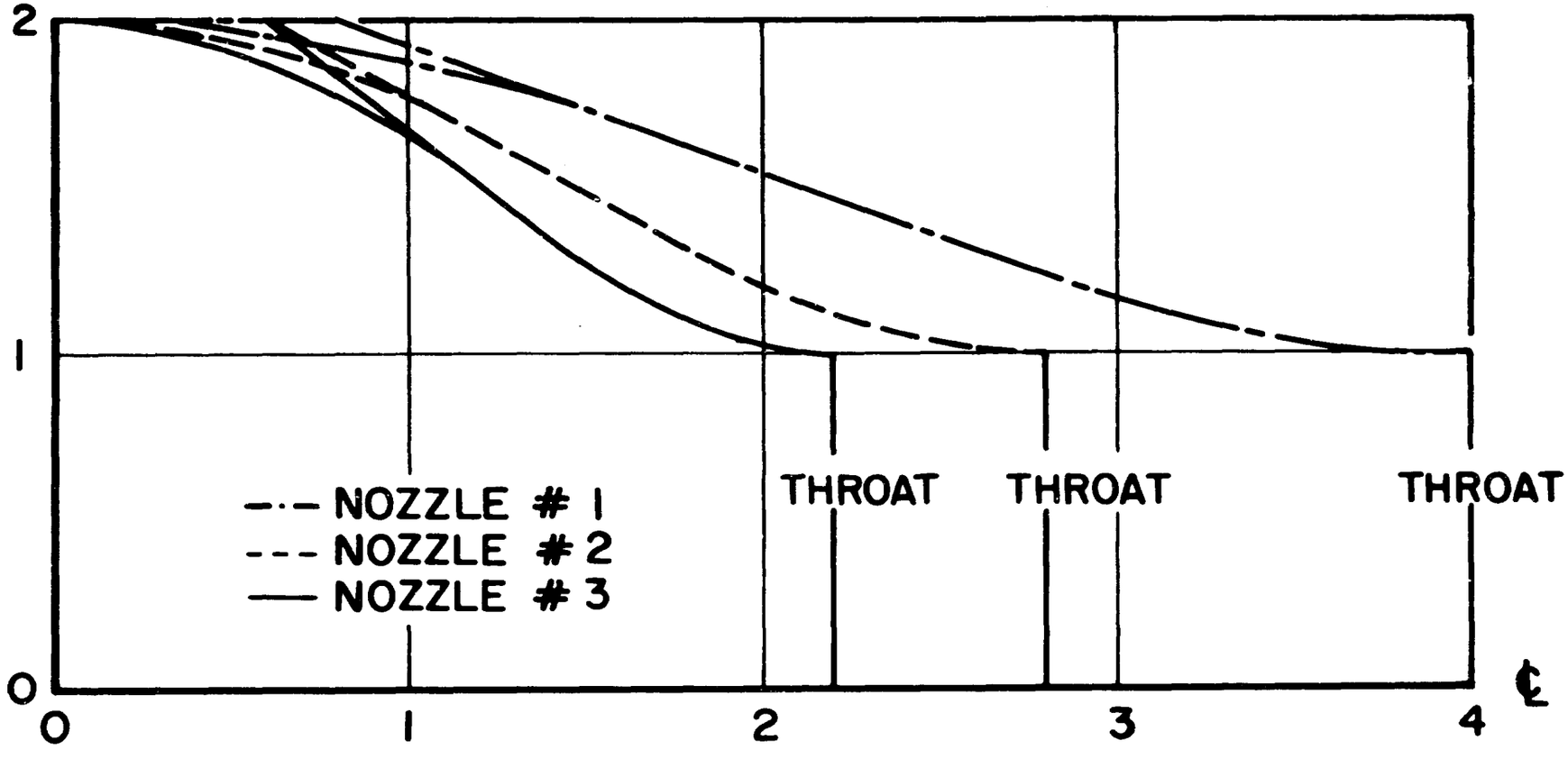

IV M3-6

Figure 6. Nozzle geometries